Sanda *et al.*: Nigerian Journal of Materials Science and Engineering. Vol. 15 (1): 1 - 6 (2025)

Structural and Thermal Characterisation of Lithium Aluminium Titanium Tantalum Phosphate NASICON-type Solid Electrolyte

[*1,2] Sanda Abubakar Sadiq, [2]Mohammed Isah Kimpa, [2]Ibrahim Sharifat Olalonpe, and [2]Isah Kasim Uthman

[1] Department of Physics, Faculty of Natural Science, Ibrahim Badamasi Babangida University Lapai, P.M.B 11 Lapai, Niger State, Nigeria.

[2] Department of Physics, School of Physical Sciences, Federal University of Technology Minna, P.M.B 65 Minna, Niger State, Nigeria.

**Corresponding: assanda@ibbu.edu.ng*

Abstract

The material with NASICON-type structure lithium aluminium titanium phosphate with tantalum substituting titanium $Li_{1.3}Al_{0.3}Ti_{1.66}Ta_{0.04}(PO_4)_3$ (LATTaP) has been synthesised via the solid-state method at a sintering temperature of 900 ºC for 6 h. The thermal analysis indicated that the reaction of the chemical mixture becomes stable around 717 ºC, indicating an improvement in the material densification. FTIR shows the presence of NASICON phosphate peaks, which were dominated by the vibration of the PO_4 ionic group. This also confirms the presence of $LiTi_2(PO_4)_3$ in all of the samples. The X-ray powder diffraction analysis shows the effect of tantalum in the composition LATTaP. The single phase has been observed due to tantalum substitution with a total conductivity of $\sigma = 1.35 \times 10^{-4}$ S/cm. These findings suggest that the composition has the potential to be used as a solid electrolyte material in lithium-ion rechargeable batteries. This material will contribute to better NASICON material for solid electrolytes.

Keywords: Solid electrolyte, $Li_{1.3}Al_{0.3}Ti_{1.66}Ta_{0.04}(PO_4)_3$, Structure, Thermal behaviour

INTRODUCTION

Lithium titanium aluminium phosphate (LATP), which possesses a NASICON-type structure, is among the most widely utilised solid electrolyte materials for solid-state battery applications. This is due to its composition of inexpensive raw materials, high ionic conductivity, broad electrochemical stability window, and ambient air stability (Yang & Wu, 2022). Consequently, solid-state batteries incorporating LATP offer the potential for high energy density; an essential attribute for applications in electric vehicles and portable electronic devices. Moreover, the material's cost-effectiveness enhances its competitiveness for large-scale production and commercial deployment (Yang *et al*., 2020).

Despite these advantages, LATP presents certain challenges in solid-state battery systems. Lithium metal, known for its exceptionally high energy density, is often considered the most favourable anode material. However, direct contact between LATP and lithium metal results in the reduction of titanium within the LATP structure, leading to interfacial degradation. This undesirable side reaction inhibits the effective utilisation of lithium metal in such systems (Oksuzoglu *et al*., 2024; Pu *et al*., 2024).

To address this issue, researchers have investigated strategies to suppress the reduction of titanium by doping LATP with various cations. Among these, pentavalent ions such as Nb^{5+} and Ta^{5+} have shown reasonable solubility at titanium sites. However, the incorporation of such dopants, while aiding in charge neutrality, alters the concentration of Li^+ ions within the structure (Lee *et al*., 2023). Notably, prior studies have provided limited insight into the thermal and structural characteristics of LATP doped with tantalum (LATTaP).

In this study, a series of characterisation techniques were employed to analyse the thermal behaviour of the material from room temperature up to 1000 °C, and to investigate its stability upon the substitution of titanium with tantalum. Additionally, the phase composition, crystal structure, microstructure, and electrical properties of the samples sintered at 900 °C were examined.

EXPERIMENTAL PROCEDURES

The material $Li_{1.3}Al_{0.3}Ti_{1.66}Ta_{0.04}(PO_4)_3$ was prepared by solid state reaction method with a stoichiometric composition of Li_2CO_3 (98%), Al_2O_3 (98.5%), TiO_2 (99.5%), Ta_2O_5 (99.99%) and $NH_4H_2PO_4$ (98.5%), all from R & M Marketing, Essex, U.K. The materials were mixed manually in an agate mortar for 1 h to ensure homogeneity. The resulting powder was then calcined at 850 °C for 2 h, with both heating and cooling rates set at 5 °C/min using a Protherm furnace. The balanced chemical reaction is shown in Equation 1 and also the experimental procedure is shown in Figure 1. Finally, the calcined powders were ground again with a planetary mono milling machine for 5 h at 400 rpm.

$$\left(\frac{1+x}{2}\right)Li_2CO_3 + (2-x-y)TiO_2 + \left(\frac{y}{2}\right)T_{a2}O_5 + \left(\frac{x}{2}\right)Al_2O_3 + 3NH_4H_2PO_4 \xrightarrow{\Delta} Li_{1+x}Ti_{2-x-y}Ta_y\,Al_x(PO_4)_3 + 6NH_3 + \left(\frac{1+x}{2}\right)CO_3 + \left(\frac{9}{2}\right)H_2O \quad (1)$$

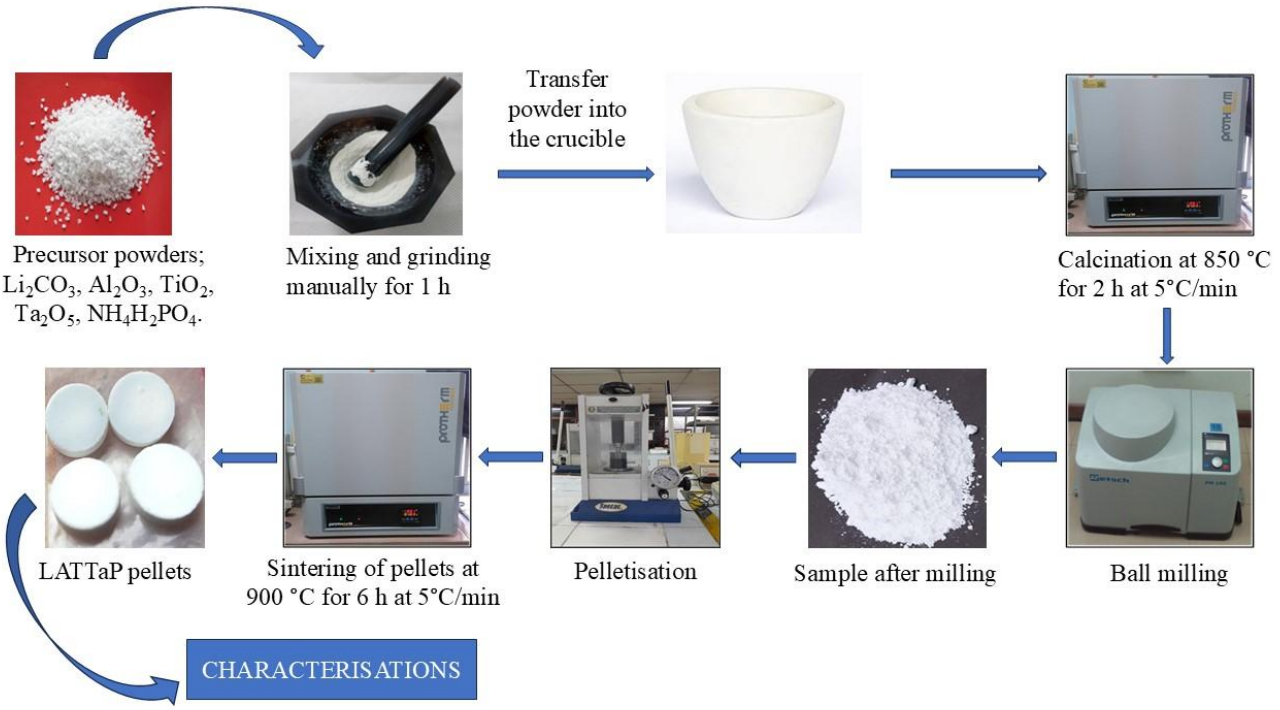

Figure 1: Experimental procedure

The as-prepared sample was characterised using the Thermogravimetric analysis method (TGA). The measurement was carried out in a Nitrogen atmosphere from 50 – 1000 °C at a heating rate of 10 °C/min. The structural compositions, microstructure and various phases of the samples LATTaP were studied and confirmed via the X-ray diffraction method (XRD) and SEM. The functional group of the sample phosphate (PO_4^{3-}) LATTaP was confirmed from the FTIR spectra. Moreover, the ionic conductivity was investigated using the impedance analysis technique.

RESULTS AND DISCUSSIONS

Figure 2 shows the thermal behaviour of $Li_{1.3}Al_{0.3}Ti_{1.66}Ta_{0.04}(PO_4)_3$ NASICON-type. It is seen from Figure 1 that the mass decreases as temperature increases, which describes the decomposition processes of the mixture. The plot is divided into five temperature regions as shown in Figure 2, with the major percentage mass loss occurring in regions I to IV, which is due to the decomposition of Li_2CO_3 and $NH_4H_2PO_4$ to evolve H_2O, NH_3 and CO_3 from the sample. As the temperature increases, the rate of mass loss decreases and becomes almost constant along region V. The thermal analysis indicated that the sample becomes stable at 717 °C.

The X-ray diffraction patterns of LATTaP powder obtained after sintering at 900 °C are shown in Figure 3. The NASICON-type phases of $LiTi_2(PO_4)_3$, with 100% corresponding to inorganic crystal structure database (ICSD) 98-006-9677 peaks, are predominantly observed in the entire patterns with space group R-3c indicating hexagonal crystal axis. The lattice parameters a = b = 8.50042 Å, c = 20.8042 Å and unit cell volume = 1301.854 Å^3 were obtained after the Rietveld analysis and compare with that in literature (Tolganbek *et al*., 2021; Wang *et al*., 2021; Sohib *et al*., 2022; Lee *et al*., 2023; Guo *et al*., 2024; Gunamony *et al*., 2024). The FTIR spectra of the as-prepared sample are shown in Figure 4, which are indicated by strong overlapping intermolecular stretching modes of vibration of PO_4^{3-} which were estimated within the range of 500 – 1300 (Taveri *et al.,* 2024). The dominant vibration band of PO_4 is within 900 – 1000 cm^{-1} in region I for a tetrahedral group, while region II and III show asymmetric bending vibration modes of O-P-O in the wavenumber range 573 - 642 cm^{-1}.

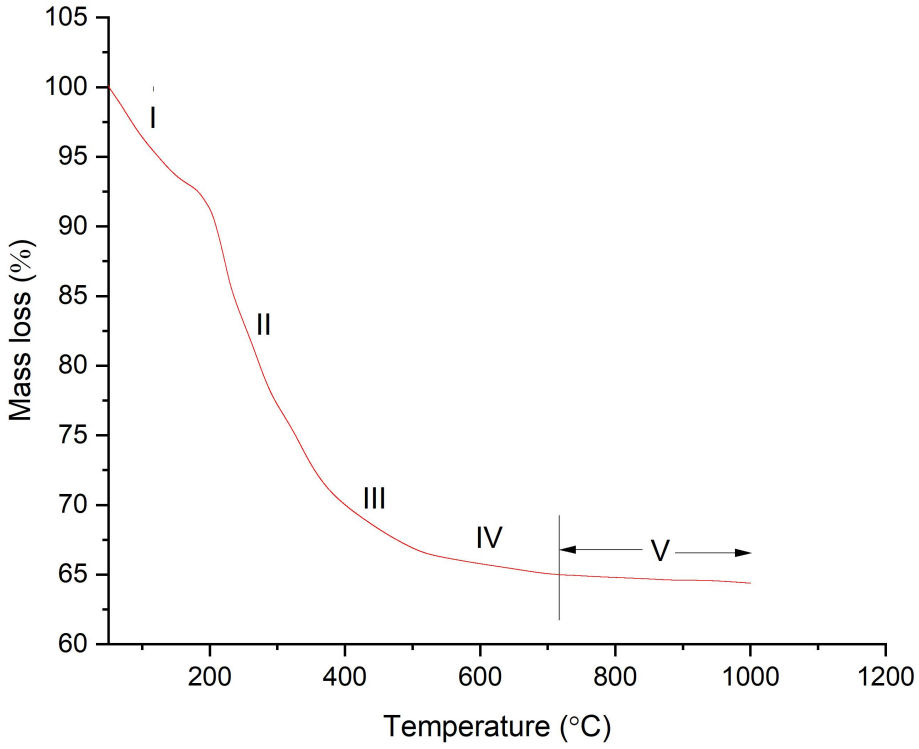

Fig. 2: TGA decomposition processes from 50 ºC to 1100 ºC of the reaction mixtures of $Li_{1.3}Al_{0.3}Ti_{1.66}Ta_{0.04}(PO_4)_3$

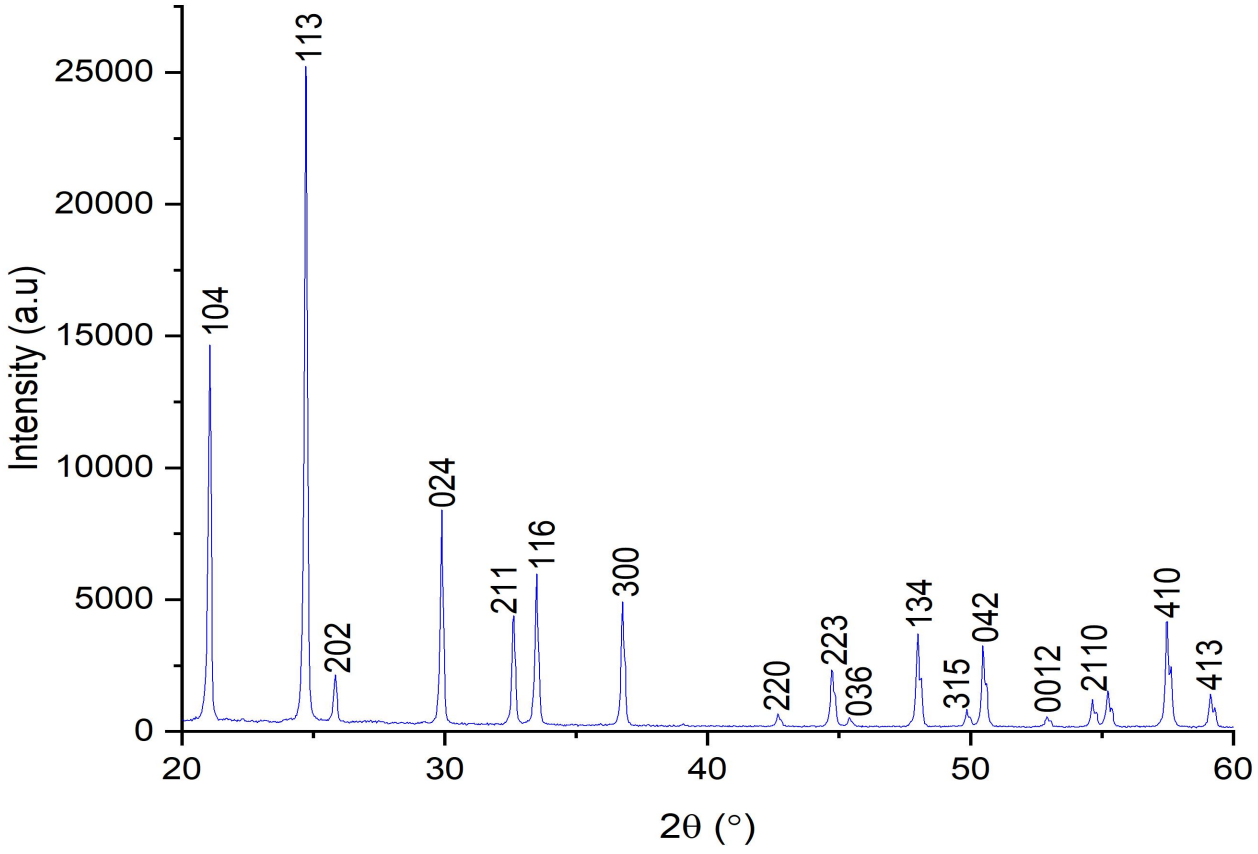

Fig. 3: XRD patterns of $Li_{1.3}Al_{0.3}Ti_{1.66}Ta_{0.04}(PO_4)_3$ sintered at 900 ºC

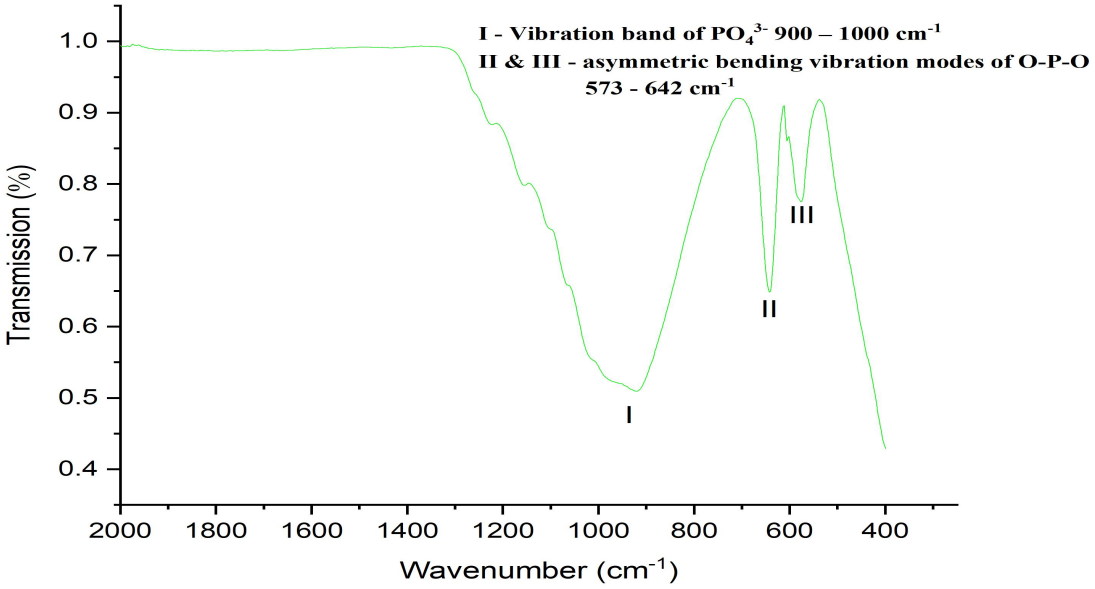

Fig. 4: FTIR spectra of $Li_{1.3}Al_{0.3}Ti_{1.66}Ta_{0.04}(PO_4)_3$ sintered at 900 ºC

Figure 5(a) shows the SEM micrographs of tantalum-substituted (LATTaP) sintered at 900 °C. Ta substitution shows that the grain morphology is cuboidal in shape with a non-uniform size distribution. These cubic-like particles are expected, showing crystallisation and consistent with the XRD data. Similar micrographs of NASICON-type composition have been reported elsewhere (Singh *et al.,* 2022; Chakraborty *et al.,* 2023). Inhomogeneity was also observed in the grain microstructure, which led to the occurrence of some pores. Thus, the porosity observed in the sample does not prevent the mobile ion movement between the grains and grain boundaries. Figure 5(b) illustrates the EDX spectrum of LATTaP sintered at 900 °C. The atomic and weight percentage of all the various elements present in the sample with the exception of Li cannot be detected by EDX machine due to the smaller size and lower atomic number.

Figure 6 presents the Nyquist plot of LATTaP sintered at 900 °C for 6 h and measured at room temperature. The spectra do not clearly resolve distinct conductive regions typically attributed to bulk and grain boundary contributions to ionic conductivity, nor do they display a well-defined low-frequency linear tail that would indicate ion-blocking behaviour at the electrode–electrolyte interface. In certain samples (particularly NASICON-type compounds containing aluminium), the separation of bulk and grain boundary responses in Nyquist representations is often difficult to discern. This is due to the close proximity in relaxation frequencies of the two contributions, resulting in overlapping semicircles, a phenomenon previously reported in the literature (Oksuzoglu *et al*., 2024; Guo *et al*., 2024).

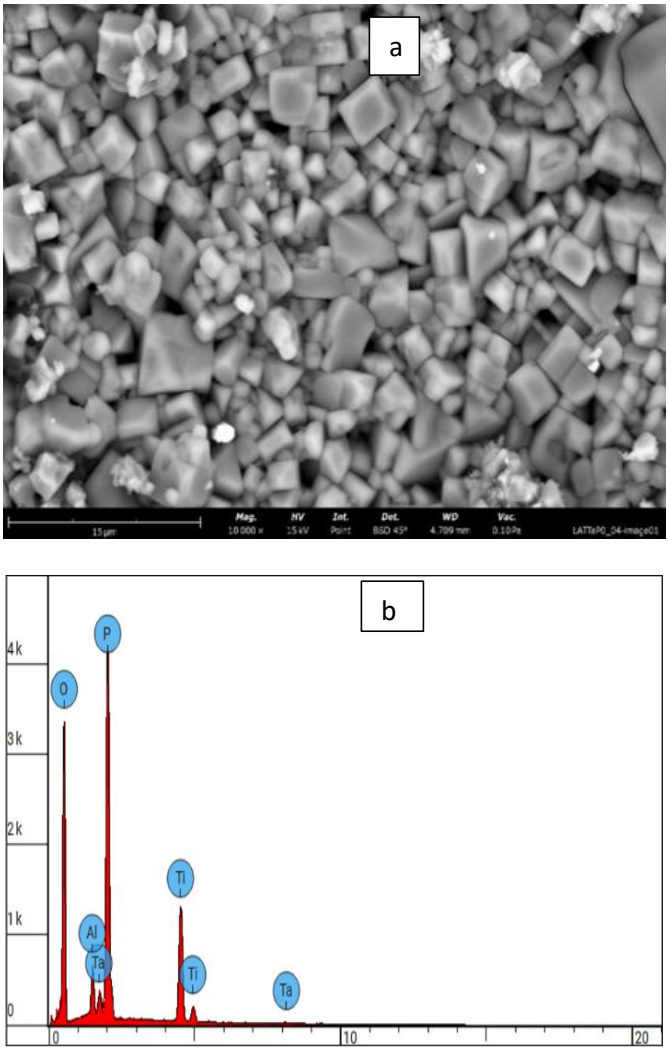

Fig. 5: (a) SEM Micrograph with Magnification 10000x of Ta substituted $Li_{1.3}Al_{0.3}Ti_{1.66}Ta_{0.04}(PO_4)_3$ sintered at 900 ºC (b) EDX spectrum indicating peaks corresponding the various elements present.

As a result, it becomes necessary to employ an electrical equivalent circuit model to deconvolute and accurately interpret the individual components of the conductivity response. The impedance spectra, recorded across the frequency range of 0.001 Hz to 1 MHz, were analysed using ZView software (version 4.0). The observed spectra exhibit dispersion rather than a symmetrical or depressed semicircle centred on the real axis, which suggests a Cole–Cole type empirical response in the Nyquist plot.

To interpret these Nyquist diagrams, the impedance data were fitted with appropriate equivalent circuits, as illustrated in the inset of Figure 6. The experimental and calculated values of the real part of the impedance (Z') were analysed as a function of angular frequency for different LATTaP compositions at room temperature. The direct current (DC) conductivity (σ) was determined using the equation $\sigma = L/RA$, where σ is the conductivity, L is the sample thickness, R is the resistance obtained from the x-axis intercept of the impedance plot, and A is the cross-sectional area of the sample.

The total ionic conductivity of LATTaP obtained in this study was 1.35×10^{-4} S cm^{-1}. Notably, this value is consistent with those reported in previous studies (Wang *et al.*, 2021; Lee *et al.*, 2023; Guo *et al.*, 2024), as summarised in Table 1.

Table 1 presents the total ionic conductivity at room temperature for LATP solid electrolytes doped with various elements. While Ta doping contributes to chemical and interfacial stability in LATP-based solid electrolytes, its impact on conductivity is less favourable compared to dopants like W and Si. The findings underscore the trade-off between stability and ionic transport performance, and highlight the importance of judicious dopant selection in optimising solid electrolyte materials for solid-state battery applications.

Table 1: Room temperature total conductivity of LATP-doped solid electrolytes

S/N	Elemental doping	RT total conductivity (S/cm)	References
1	Si	1.00 x 10^{-3}	Zhu *et al.*, 2022
2	Te	7.03 x 10^{-4}	Wang *et al.*, 2021
3	Sn	4.71 x 10^{-4}	Xu *et al.*, 2022
4	Cl	4.23 x 10^{-4}	Li *et al.*, 2021
5	W	1.186 x 10^{-3}	Guo *et al.*, 2024
6	Ta	1.91 x 10^{-4}	Lee *et al.*, 2023
7	Ta	1.39 x 10^{-4}	This study

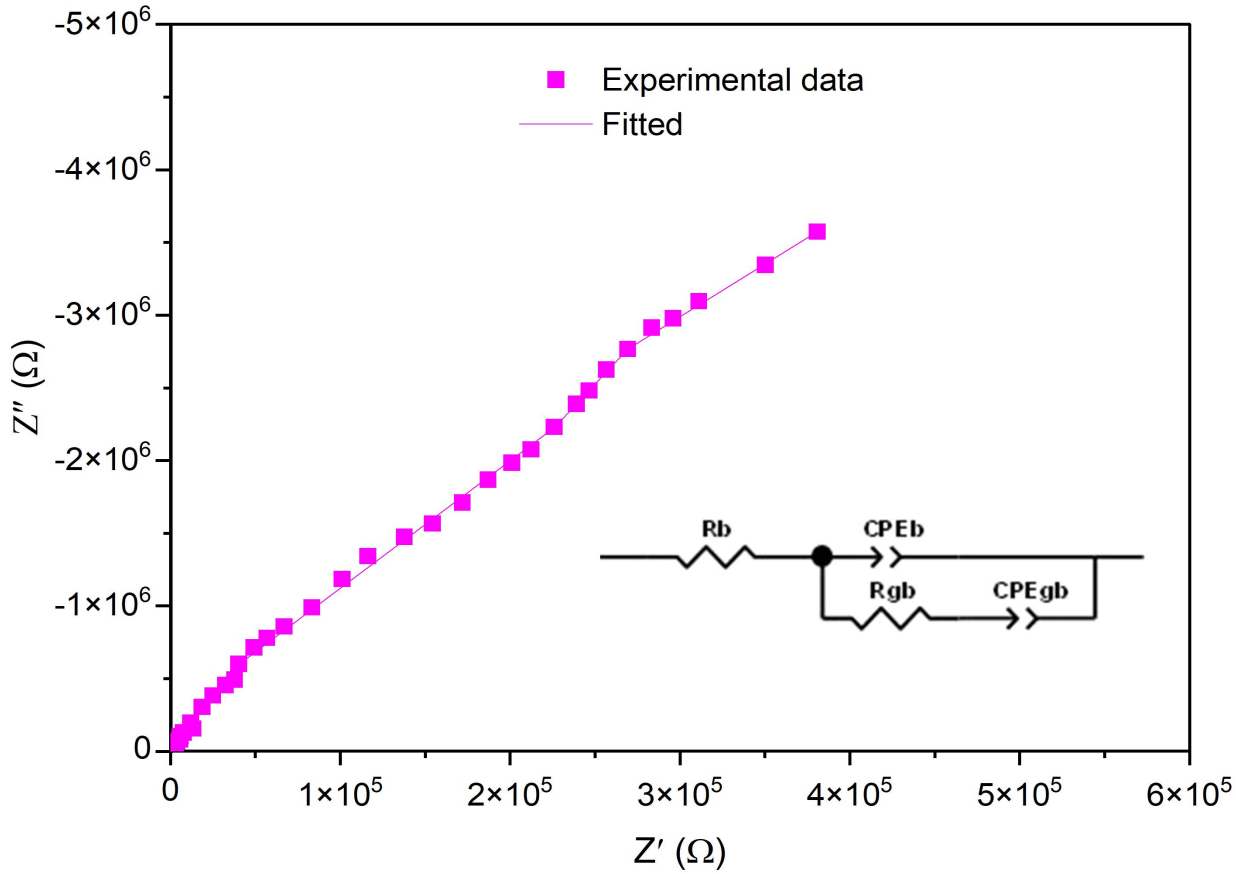

Figure 6: Nyquist plot of $Li_{1.3}Al_{0.3}Ti_{1.66}Ta_{0.04}(PO_4)_3$ sintered at 900 ºC with fitted equivalent circuit

CONCLUSION

The material was successfully synthesized with ICSD card no 98-006-9677 with single phase. The thermal analysis indicated that the LATTaP becomes stable at 717 ºC. The micrograph of Ta substituted LATTaP indicated cubic-like shape with non-uniform size distribution. The sample showed total conductivity σ = 1.35 x 10^{-4} Scm^{-1}. This composition has potential to be used as solid electrolyte material in lithium-ion rechargeable batteries. This material will contribute to better NASICON material for solid electrolytes.

ACKNOWLEDGMENT

This work was financially supported by the Tertiary Education Trust Fund (TETFund) through Ibrahim Badamasi Babangida University Lapai. The authors gratefully acknowledge the Department of Physics, Faculty of Science, Universiti Putra Malaysia (UPM) for the facilities provided.

REFERENCES

Chakraborty, A., Thirupathi, R., Bhattacharyya, S., Singh, K., & Omar, S. (2023). Mg-doped NASICON-type electrolyte for rechargeable solid-state sodium-ion batteries. *Journal of Power Sources*, 572, 1 – 15.

Gunamony, J., Walle, K. Z., & Kotobuki, M. (2024). Influence of mixing technique on properties of $Li_{1.3}Al_{0.3}Ti_{1.7}(PO_4)_3$ solid electrolyte prepared by the solid-state reaction A comparison of dry 3D mixing technique with wet ball-milling, Solid State Ionics, 410, 1 – 10.

Guo, Y., Zhao, E., & Li, J. (2024). Superior ionic conductivity of W-doped NASICON-type $Li_{1.3}Al_{0.3}Ti_{1.7}(PO_4)_3$ solid electrolyte. *Journal of the European Ceramic Society*, *44*(12), 7081–7091.

Lee, J., Wook Lee, Y., Shin, S., Ho Shin, T., & Lee, S. (2023). Interface characteristics of $Li_{1+x}Al_xTi_{2-x}(PO_4)_3$ solid electrolyte with Ta-doping for All-Solid-State batteries. *Inorganic Chemistry Communications*, 154: 1-6.

Li, S. Y., Huang, Z. Y., Xiao, Y. G., & Sun, W. C. (2021). Chlorine-doped $Li_{1.3}Al_{0.3}Ti_{1.7}(PO_4)_3$ as an electrolyte for solid lithium metal batteries. *Material Chemistry Frontier*, 5: 5336 – 5343.

Oksuzoglu, F., Ates, S., Ozkendir, O. M., Celik, G., Eker, Y. R., & Baveghar, H. (2024). Structure and ionic conductivity of NASICON-type LATP solid electrolyte synthesized by the solid-state method. *Ceramics International*, 50(17), 31435 - 31441.

Pu, X., Cheng, X., Yan, Q., Lin, Y., Yan, R., Yang, R., & Zhu, X. (2024). NASICON-type Ta^{5+} substituted $LiZr_2(PO_4)_3$ with improved ionic conductivity as a prospective solid electrolyte. *Ceramics International*, 50(6), 9007 - 9015.

Singh, K., Chakraborty, A., Thirupathi, R. (2022). Recent advances in NASICON-type oxide electrolytes for solid-state sodium-ion rechargeable batteries. *Ionics* 28, 5289–5319.

Sohib, A., Karunawan, J., Sundari, C.D., Floweri, O., & Iskandar, F. (2022). Rietveld study on the effect of pelletizing and sintering towards the structural evolution of $Li_{1.3}Al_{0.3}Ti_{1.7}(PO_4)_3$. *Journal of Physics: Conference Series,* 1 – 8.

Taveri, G., Güneren, A., Barlog, M., Hnatko, M., Zhukova, I., Netriova, Z., Simon, E., Micusik, M., Mikolasek, M., & Karkova, H. (2024). Understanding the benefits of Al^{3+}-doping on NaSICONs explained through an out-of-the-scheme isovalent substitution of Fe^{3+} in $Na_3Fe_2(PO_4)_3$ series. *Journal of Power Sources*, 592, 1 -12.

Tolganbek, N., Yerkinbekova, Y., Kahirullin, A., Bakenov, Z., Kanamura, K., & Mentbayeva, A. (2021). Enhancing purity and ionic conductivity of NASICON-typed $Li_{1.3}Al_{0.3}Ti_{1.7}(PO_4)_3$ solid electrolyte. *Ceramics International.* 47(13): 18188 – 18195.

Wang, Q. H., Liu, L., Zhao, B. J., Zhang, L., Xiao, X., Yan, H., Xu, G. L., Ma, L., Liu, Y. (2021). Transport and interface characteristics of Te-doped NASICON solid electrolyte $Li_{1.3}Al_{0.3}Ti_{1.7}(PO_4)_3$. *Electrochimica Acta*, 399: 1 – 11.

Xu, A., Wang, R., Yao, M., Cao, J., Li, M., Yang, C., Liu, F., & Ma, J. (2022). Electrochemical Properties of an Sn-Doped LATP Ceramic Electrolyte and Its Derived Sandwich-Structured Composite Solid Electrolyte. *Nanomaterials*. 12(12): 2082.

Yang, H., & Wu, N. (2022). Ionic conductivity and ion transport mechanisms of solid-state lithium-ion battery electrolytes: a review, *Energy Science and Engineering*. 10 (5): 1643 – 1671.

Yang, Z., Yuan, H., Zhou, C., Wu, Y., Tang, W., Sang, S., & Liu, H. (2020). Facile interfacial adhesion enabled LATP-based solid-state lithium metal battery, *Chemical Engineering Journal.* 392: 1 – 7.

Zhu, J., Xiang, Y., Zhao, J., Wang, H., Li, Y., Zheng, B., He, H., Zhang, Z., Huang, J., & Yang, Y. (2022). Insights into the local structure, microstructure and ionic conductivity of silicon doped NASICON-type solid electrolyte $Li_{1.3}Al_{0.3}Ti_{1.7}P_3O_{12}$. *Energy Storage Materials*, *44*, 190–196.